MULTIANTENNA DETECTION OF CONSTANT-ENVELOPE SIGNALS IN NOISE OF UNKNOWN VARIANCE

Daniel Romero and Roberto Lopez-Valcarce

Department of Signal Theory and Communications, Universidade de Vigo, 36310 Vigo, Spain
email: {dromero, valcarce}@gts.uvigo.es

ABSTRACT

Detection of unknown signals with constant modulus (CM) using multiple antennas in additive white Gaussian noise of unknown variance is considered. The channels from the source to each antenna are assumed frequency-flat and unknown. This problem is of interest for spectrum sensing in cognitive radio systems in which primary signals are known to have the CM property. Examples include analog frequency modulated signals such as those transmitted by wireless microphones in the TV bands and Gaussian Minimum Shift Keying modulated signals as in the GSM cellular standard. The proposed detector, derived from a Generalized Likelihood Ratio (GLR) approach, exploits both the CM property and the spatial independence of noise, outperforming the GLR test for Gaussian signals as shown by simulation.

Index Terms— Cognitive radio, spectrum sensing, detection, constant modulus.

1. INTRODUCTION

Nowadays, the shortage of spectrum resources conflicts with the widespread presence of wireless communication services. However, the fact that significant parts of the licensed spectrum remain unused for long periods of time is motivating the concept of opportunistic (unlicensed) spectrum access, which is an important ingredient of the Cognitive Radio paradigm [1]. Its implementation calls for powerful spectrum sensing algorithms in order to detect transmissions from primary (licensed) users and avoid interference. The design of these schemes is challenged by the fact that, in order to overcome the hidden node problem, primary signals have to be detected at low Signal-to-Noise Ratios (SNR) that do not allow their decodability. Thus, primary signal features requiring time or frequency synchronization in order to be revealed (pilot symbols, spreading sequences, etc.) are difficult to exploit, and detection schemes able to work with asynchronously sampled waveforms are clearly desirable.

In some cases of practical interest, primary transmissions take place by means of *constant magnitude* (CM) waveforms. For instance, wireless microphones operating in the TV bands, which must be protected under the rules set forth by the Federal Communications Commission (FCC) [3], typically employ analog Frequency Modulation (FM). In addition, CM waveforms are desirable for portable digital radios due to the reduced power amplifier backoff needed and consequent increase in power efficiency and decrease in handset dc power requirements and physical size; the Gaussian Minimum Shift Keying (GMSK) modulation employed by the GSM cellular system is an important example. Other CM modulation schemes include Frequency Shift Keying (FSK) and Continuous Phase Modulation (CPM).

The CM property is a strong waveform feature that has long been exploited in equalization [4] and array processing [5]. More recently, it has been considered in [6] in a signal detection context, where a detector was developed for unknown CM signals immersed in Gaussian noise of unknown variance. This is relevant since many popular spectrum sensing methods, such as the Energy Detector [7], are quite sensitive to uncertainties about the background noise level [8]. In addition, the CM property of a waveform is invariant to carrier offsets and sampling jitter, clearly an appealing feature.

Another means to combat noise uncertainty is to exploit the spatial independence of the noise when multiple antennas are available. Most multiantenna detectors in the literature adopt a Gaussian model for the signal of interest [10, 11]. Therefore, it is reasonable to ask whether the performance of these multiantenna schemes can be improved by taking the CM property of the signal into account. Our goal is to extend the Generalized Likelihood Ratio (GLR) detector from [6] to multiple antenna sensors, so that the CM signal property and the spatial independence of the noise can be jointly exploited.

In Sec. 2 the system model is presented; the GLR detector is derived in Secs. 3 and 4. Simulations are provided in Sec. 5, and conclusions are drawn in Sec. 6.

2. SYSTEM MODEL

Consider a cognitive node with M antennas, in which the received signals are downconverted to baseband and sampled.

Work supported by the Spanish Government and the European Regional Development Fund (ERDF) under projects DYNACS (TEC2010-21245-C02-02/TCM) and COMONSENS (CONSOLIDER-INGENIO 2010 CSD2008-00010).

In this way, K complex-valued samples from each antenna are gathered in the rows of the $K \times M$ matrix $\boldsymbol{Y}$. Assume that the bandwidth of the signal is smaller than the coherence bandwidth of the channel so that the latter can be assumed frequency flat. In the presence of a constant-envelope primary transmission, the matrix of observations is given by $\boldsymbol{Y} = \boldsymbol{x}(\boldsymbol{\phi})\boldsymbol{h}^H + \sigma\boldsymbol{W}$, where $\boldsymbol{W}$ is a $K \times M$ matrix of noise samples, assumed zero-mean circular Gaussian, spatially and temporally white with unit variance, so that $E\{\boldsymbol{W}_{ki}\boldsymbol{W}_{lj}^*\} = \delta_{kl}\delta_{ij}$. The (unknown) noise variance at each antenna is σ^2. The vector of channel gains is denoted by $\boldsymbol{h}^*$, and $\boldsymbol{x}(\boldsymbol{\phi}) = [\ e^{j\phi_1} \quad e^{j\phi_2} \quad \cdots \quad e^{j\phi_K}\ ]^T$ is the CM signal vector. Similarly to [6], the phases $\phi_k \in [0, 2\pi)$ are assumed deterministic and constitute additional unknown nuisance parameters.

Therefore, the hypothesis testing problem is stated as

$$\begin{array}{lll} \mathcal{H}_0 & : & \boldsymbol{Y} = \sigma\boldsymbol{W}, \\ \mathcal{H}_1 & : & \boldsymbol{Y} = \boldsymbol{x}(\boldsymbol{\phi})\boldsymbol{h}^H + \sigma\boldsymbol{W}, \end{array} \tag{1}$$

with $\boldsymbol{h}$, $\boldsymbol{\phi}$, σ^2 unknown.

The observations are conditionally Gaussian under both hypotheses. Under $\mathcal{H}_0$, the pdf of $\boldsymbol{Y}$ is given by

$$p(\boldsymbol{Y}; \sigma^2 \,|\, \mathcal{H}_0) = \left[\frac{1}{(\pi\sigma^2)^M} \exp\left\{-\frac{1}{\sigma^2}\operatorname{tr}\{\hat{\boldsymbol{R}}_0\}\right\}\right]^K \tag{2}$$

where $\hat{\boldsymbol{R}}_0 \doteq \frac{1}{K}\boldsymbol{Y}^H\boldsymbol{Y}$. On the other hand, under $\mathcal{H}_1$, the pdf is

$$p(\boldsymbol{Y}; \sigma^2, \boldsymbol{\phi}, \boldsymbol{h} \,|\, \mathcal{H}_1) = \left[\frac{1}{(\pi\sigma^2)^M} \exp\left\{-\frac{1}{\sigma^2}\operatorname{tr}\{\hat{\boldsymbol{R}}_1\}\right\}\right]^K \tag{3}$$

where now $\hat{\boldsymbol{R}}_1 \doteq \frac{1}{K}[\boldsymbol{Y} - \boldsymbol{x}(\boldsymbol{\phi})\boldsymbol{h}^H]^H[\boldsymbol{Y} - \boldsymbol{x}(\boldsymbol{\phi})\boldsymbol{h}^H]$.

3. DERIVATION OF THE GLR TEST

The GLR test [7] can be summarized as

$$L_G(\boldsymbol{Y}) \doteq \frac{\max_{\sigma^2,\boldsymbol{\phi},\boldsymbol{h}} p(\boldsymbol{Y}; \sigma^2, \boldsymbol{\phi}, \boldsymbol{h} \,|\, \mathcal{H}_1)}{\max_{\sigma^2} p(\boldsymbol{Y}; \sigma^2 \,|\, \mathcal{H}_0)} \underset{\mathcal{H}_0}{\overset{\mathcal{H}_1}{\gtrless}} \gamma \tag{4}$$

where γ is a threshold whose value is usually set in order to satisfy some false alarm rate requirement. Thus, the Maximum Likelihood (ML) estimates of the nuisance parameters under each hypothesis must be obtained.

3.1. ML estimates under $\mathcal{H}_0$

The ML estimate of σ^2 under $\mathcal{H}_0$ is given by

$$\begin{aligned} \hat{\sigma}_0^2 &= \arg\max_{\sigma^2} p(\boldsymbol{Y}; \sigma^2 \,|\, \mathcal{H}_0) \\ &= \frac{1}{M}\operatorname{tr}\{\hat{\boldsymbol{R}}_0\}, \end{aligned} \tag{5}$$

and therefore,

$$p(\boldsymbol{Y}; \hat{\sigma}_0^2 \,|\, \mathcal{H}_0) = \left[\frac{\pi e}{M}\operatorname{tr}\{\hat{\boldsymbol{R}}_0\}\right]^{-MK}. \tag{6}$$

3.2. ML estimates under $\mathcal{H}_1$

Similarly to (5), the ML estimate of σ^2 under $\mathcal{H}_0$ is

$$\hat{\sigma}_1^2 = \frac{1}{M}\operatorname{tr}\{\hat{\boldsymbol{R}}_1\} \tag{7}$$

which yields

$$p(\boldsymbol{Y}; \hat{\sigma}_1^2, \boldsymbol{\phi}, \boldsymbol{h} \,|\, \mathcal{H}_1) = \left[\frac{\pi e}{M}\operatorname{tr}\{\hat{\boldsymbol{R}}_1\}\right]^{-MK}. \tag{8}$$

Now the ML estimate of $\boldsymbol{\phi}$ under $\mathcal{H}_1$ is that minimizing $tr\{\hat{\boldsymbol{R}}_1\}$, or, equivalently,

$$\hat{\boldsymbol{\phi}} = \arg\max_{\boldsymbol{\phi}} \operatorname{Re}\left\{\boldsymbol{x}^H(\boldsymbol{\phi})\boldsymbol{Y}\boldsymbol{h}\right\}. \tag{9}$$

Partitioning $\boldsymbol{Y}$ row-wise as

$$\boldsymbol{Y} = \begin{bmatrix} \boldsymbol{y}_1^H \\ \boldsymbol{y}_2^H \\ \vdots \\ \boldsymbol{y}_K^H \end{bmatrix}, \tag{10}$$

it is clear that (9) becomes

$$\hat{\boldsymbol{\phi}} = \arg\max_{\boldsymbol{\phi}} \operatorname{Re}\left\{\sum_{k=1}^K e^{-j\phi_k}\boldsymbol{y}_k^H\boldsymbol{h}\right\}, \tag{11}$$

so that

$$\hat{\phi}_k = \angle\left(\boldsymbol{y}_k^H\boldsymbol{h}\right). \tag{12}$$

With this, one has

$$\operatorname{Re}\left\{\boldsymbol{x}^H(\hat{\boldsymbol{\phi}})\boldsymbol{Y}\boldsymbol{h}\right\} = ||\boldsymbol{Y}\boldsymbol{h}||_1, \tag{13}$$

where $||\cdot||_1$ denotes the ℓ^1-norm. Substituting (13) back in (8) gives

$$\begin{aligned} &p(\boldsymbol{Y}; \hat{\sigma}_1^2, \hat{\boldsymbol{\phi}}, \boldsymbol{h} \,|\, \mathcal{H}_1) \\ &= \left[\frac{\pi e}{MK}\left(\operatorname{tr}\{\boldsymbol{Y}^H\boldsymbol{Y}\} - 2||\boldsymbol{Y}\boldsymbol{h}||_1 + K||\boldsymbol{h}||_2^2\right)\right]^{-MK} \end{aligned} \tag{14}$$

Maximizing (14) w.r.t. $\boldsymbol{h}$ returns the ML estimate $\hat{\boldsymbol{h}}$. To do so, let us write $\boldsymbol{h} = \alpha \cdot \boldsymbol{g}$, where $\alpha > 0$ and $||\boldsymbol{g}||_2 = 1$. The value of α maximizing (14) is readily found to be

$$\hat{\alpha} = \frac{1}{K}||\boldsymbol{Y}\boldsymbol{g}||_1. \tag{15}$$

After substitution of $\hat{\alpha}$ in (14), the ML estimate of the spherical component $\boldsymbol{g}$ is seen to be

$$\hat{\boldsymbol{g}} = \arg\max_{\boldsymbol{g}} ||\boldsymbol{Y}\boldsymbol{g}||_1 \quad \text{s.t.} \quad ||\boldsymbol{g}||_2 = 1. \tag{16}$$

Although this problem cannot be solved in closed form, in Sec. 4 we present a computationally efficient iterative method that generally obtains reasonably good solutions.

Finally, the likelihood function becomes:

$$\begin{aligned} &p(\boldsymbol{Y}; \hat{\sigma}_1^2, \hat{\boldsymbol{\phi}}, \hat{\alpha}, \hat{\boldsymbol{g}} \,|\, \mathcal{H}_1) \\ &= \left[\frac{\pi e}{MK}\left(\operatorname{tr}\{\boldsymbol{Y}^H\boldsymbol{Y}\} - \frac{1}{K}||\boldsymbol{Y}\hat{\boldsymbol{g}}||_1^2\right)\right]^{-MK} \end{aligned} \tag{17}$$

3.3. GLR test

Combining (6) and (17) with (4), the GLR test is obtained:

$$L_G(\boldsymbol{Y}) = \left[\frac{\operatorname{tr}\{\boldsymbol{Y}^H\boldsymbol{Y}\}}{\operatorname{tr}\{\boldsymbol{Y}^H\boldsymbol{Y}\} - \frac{1}{K}||\boldsymbol{Y}\hat{\boldsymbol{g}}||_1^2}\right]^{MK}. \tag{18}$$

Note that the bracketed term is an increasing function of $||\boldsymbol{Y}\hat{\boldsymbol{g}}||_1^2/\operatorname{tr}\{\boldsymbol{Y}^H\boldsymbol{Y}\}$ and that $\operatorname{tr}\{\boldsymbol{Y}^H\boldsymbol{Y}\} = ||\boldsymbol{Y}||_F^2$, where $||\cdot||_F$ denotes the Frobenius norm. This allows us to rewrite the test more compactly as

$$L_1(\boldsymbol{Y}) \doteq \frac{||\boldsymbol{Y}\hat{\boldsymbol{g}}||_1}{||\boldsymbol{Y}||_F} \underset{\mathcal{H}_0}{\overset{\mathcal{H}_1}{\gtrless}} \gamma'. \tag{19}$$

where $\gamma' = \sqrt{1-\gamma^{-MK/2}}$. Note that for a single antenna ($M = 1$), this GLR test reduces to the one in [6].

4. ML ESTIMATION OF THE CHANNEL VECTOR

In this section we analyze in detail the constrained maximization problem (16). The analysis will lead to an efficient iterative algorithm to search for a maximum of the cost, which can be written explicitly as

$$\begin{aligned} J(\boldsymbol{g}) = ||\boldsymbol{Y}\boldsymbol{g}||_1 &= \sum_{k=1}^{K} |\boldsymbol{y}_k^H\boldsymbol{g}| \\ &= \sum_{k=1}^{K} \sqrt{\boldsymbol{g}^H\boldsymbol{y}_k\boldsymbol{y}_k^H\boldsymbol{g}}. \end{aligned} \tag{20}$$

Thus we must maximize (20) subject to $\boldsymbol{g}^H\boldsymbol{g} = 1$. The corresponding Lagrangian for this problem is

$$\mathcal{L}(\boldsymbol{g},\lambda) \doteq J(\boldsymbol{g}) - \frac{\lambda}{2}(\boldsymbol{g}^H\boldsymbol{g} - 1). \tag{21}$$

Note that the gradient of the constraint is $2\boldsymbol{g}$, which does not vanish on the unit sphere $||\boldsymbol{g}||_2 = 1$. Hence all feasible points are regular, and any local extremum of the constrained problem must satisfy the first-order necessary conditions

$$\nabla_{\boldsymbol{g}}\mathcal{L}(\boldsymbol{g},\lambda) = 0, \qquad \nabla_{\lambda}\mathcal{L}(\boldsymbol{g},\lambda) = 0, \tag{22}$$

which are readily seen to yield

$$\nabla_{\boldsymbol{g}} J(\boldsymbol{g}) = \lambda\boldsymbol{g}, \qquad \boldsymbol{g}^H\boldsymbol{g} = 1. \tag{23}$$

The gradient of J is given by

$$\begin{aligned} \nabla_{\boldsymbol{g}} J(\boldsymbol{g}) &= \sum_{k=1}^{K} \frac{\boldsymbol{y}_k\boldsymbol{y}_k^H}{|\boldsymbol{y}_k^H\boldsymbol{g}|}\boldsymbol{g} \\ &= \boldsymbol{A}(\boldsymbol{g})\cdot\boldsymbol{g}, \end{aligned} \tag{24}$$

where we have introduced the $M \times M$ matrix

$$\boldsymbol{A}(\boldsymbol{g}) \doteq \sum_{k=1}^{K} \frac{\boldsymbol{y}_k\boldsymbol{y}_k^H}{|\boldsymbol{y}_k^H\boldsymbol{g}|} = \boldsymbol{Y}^H\boldsymbol{D}^{-1}(\boldsymbol{g})\boldsymbol{Y}, \tag{25}$$

where

$$\boldsymbol{D}(\boldsymbol{g}) \doteq \begin{bmatrix} |\boldsymbol{y}_1^H\boldsymbol{g}| & & \\ & \ddots & \\ & & |\boldsymbol{y}_K^H\boldsymbol{g}| \end{bmatrix}. \tag{26}$$

Note that $\boldsymbol{A}(\boldsymbol{g})$ is positive (semi)definite, and that the cost (20) can be written as

$$J(\boldsymbol{g}) = \boldsymbol{g}^H\boldsymbol{A}(\boldsymbol{g})\boldsymbol{g}. \tag{27}$$

Substituting (24) into (23) yields

$$\boldsymbol{A}(\boldsymbol{g})\boldsymbol{g} = \lambda\boldsymbol{g}, \qquad \boldsymbol{g}^H\boldsymbol{g} = 1. \tag{28}$$

Thus we see that at any extremum of the constrained problem, $\boldsymbol{g}$ must be a unit-norm eigenvector of $\boldsymbol{A}(\boldsymbol{g})$. The corresponding eigenvalue is the value of the attained cost, i.e. $J(\boldsymbol{g}) = \boldsymbol{g}^H\boldsymbol{A}(\boldsymbol{g})\boldsymbol{g} = \lambda$. Note that these conditions do not reveal whether λ corresponds to the largest, smallest, or an intermediate eigenvalue of $\boldsymbol{A}(\boldsymbol{g})$. However, by examining the high SNR case, for which $\boldsymbol{Y} \approx \boldsymbol{x}\boldsymbol{h}^H$, one sees that

$$\begin{aligned} \boldsymbol{A}(\boldsymbol{g}) &= \boldsymbol{Y}^H\boldsymbol{D}^{-1}(\boldsymbol{g})\boldsymbol{Y} \\ &\approx [\boldsymbol{x}^H\boldsymbol{D}^{-1}(\boldsymbol{g})\boldsymbol{x}]\boldsymbol{h}\boldsymbol{h}^H, \end{aligned} \tag{29}$$

i.e. a rank-1 matrix, whose eigenvector associated to the largest eigenvalue is the true channel vector $\boldsymbol{h}$ (independently of $\boldsymbol{g}$). Therefore, it makes sense to consider numerical methods for the computation of the principal eigenvector of a matrix, and then update the matrix at each iteration by using the eigenvector estimate from the previous step. For example, the standard power method [9] can be suitably modified in this manner, yielding Algorithm 1.

A reasonable initializer for any numerical method of this kind is the eigenvector associated to the largest eigenvalue of $\boldsymbol{Y}^H\boldsymbol{Y}$, since this is the solution to (16) if we relax the ℓ^1-norm to the ℓ^2-norm in the cost function. In addition, since all elements of $\boldsymbol{x}$ have unit magnitude, in the high SNR regime one has $\boldsymbol{D}(\boldsymbol{g}) \approx |\boldsymbol{h}^H\boldsymbol{g}|\boldsymbol{I}$, so that

$$\boldsymbol{A}(\boldsymbol{g}) \approx \frac{1}{|\boldsymbol{h}^H\boldsymbol{g}|}\boldsymbol{Y}^H\boldsymbol{Y}, \tag{30}$$

and thus the eigenvectors of $\boldsymbol{A}(\boldsymbol{g})$ and $\boldsymbol{Y}^H\boldsymbol{Y}$ should lie close to each other.

Algorithm 1 Modified Power Method

Set $\boldsymbol{g}_0$ = principal eigenvector of $\boldsymbol{Y}^H\boldsymbol{Y}$
for $k = 0$ to $n\_\text{iter} - 1$ **do**
  $\boldsymbol{v}_{k+1} = \boldsymbol{A}(\boldsymbol{g}_k)\boldsymbol{g}_k$
  $\boldsymbol{g}_{k+1} = \dfrac{\boldsymbol{v}_{k+1}}{||\boldsymbol{v}_{k+1}||_2}$
end for
Set $\hat{\boldsymbol{g}} = \boldsymbol{g}_{n\_\text{iter}}$

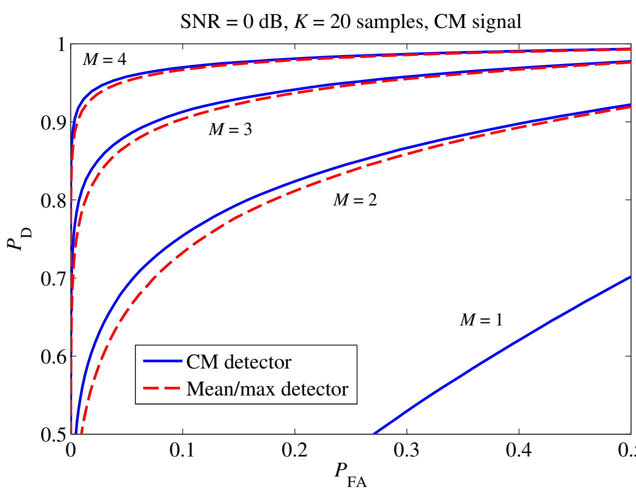

Fig. 1. ROC curves of the CM and mean/max detectors with a constant-envelope signal for different array sizes.

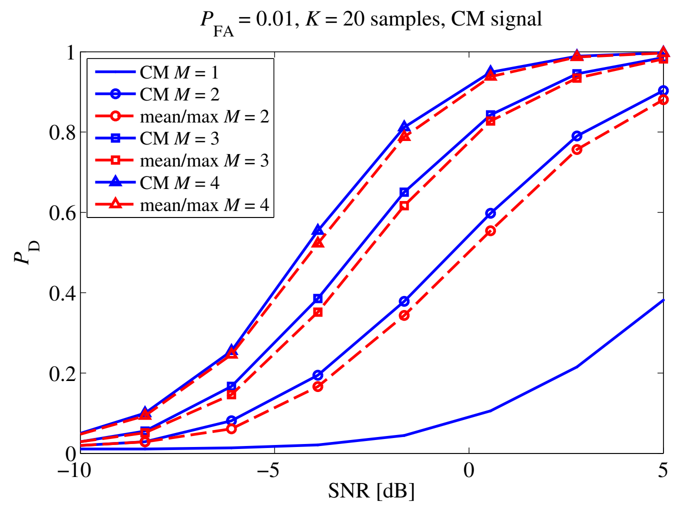

Fig. 2. Probability of detection for a fixed probability of false alarm *vs* SNR for different antenna array sizes.

5. SIMULATION RESULTS

We illustrate the performance of the proposed GLR detector by means of Monte Carlo simulation in independent Rayleigh fading channels. The number of iterations in Algorithm 1was set to 30, a value that ensured convergence in all cases tested. In fact, no performance degradation was perceived even with much fewer iterations. This is indicative that the proposed initialization works quite well in practice.

The proposed detector is compared with the GLR detector for Gaussian signals, which was derived in [10]:

$$\frac{\frac{1}{M}\operatorname{tr}\{\hat{\boldsymbol{R}}_0\}}{\lambda_1(\hat{\boldsymbol{R}}_0)} \underset{\mathcal{H}_1}{\overset{\mathcal{H}_0}{\gtrless}} \gamma'', \tag{31}$$

where $\lambda_1(\boldsymbol{P})$ denotes the largest eigenvalue of $\boldsymbol{P}$. We will refer to (31) as the "mean/max detector", and to the proposed GLR test as "CM detector".

The Receiver Operating Characteristic (ROC) curves for the two detectors are shown in Fig. 1, for different number of antennas.The phases ϕ_k in the signal vector $\boldsymbol{x}(\boldsymbol{\phi})$ were independently drawn from a uniform distribution in $[0, 2\pi)$. Note that the mean/max detector requires $M > 1$, whereas the CM detector can be used with a single antenna. Nevertheless, the performance improvement obtained when additional antennas are available is clear. The CM detector consistently outperforms the mean/max test, although this advantage becomes smaller as the number of antennas is increased. This indicates that the CM property becomes less useful for detection purposes once a large number of spatial degrees of freedom is available. This behavior can be also seen in Fig. 2, which shows the probability of detection for both schemes as a function of the SNR.

We also tested the performance of these detectors with a GMSK signal generated according to the GSM cellular standard, downconverted to baseband and I/Q sampled at 2 Msamples/s. Fig. 3 shows the power spectral density (psd) and samples in the I/Q plane of the test signal. Although GMSK is a constant-envelope modulation, it is clear from Fig. 3 that the CM property holds only approximately in practice. This is due to nonlinearities introduced by the downconversion analog stage. Despite of this effect, it is seen in Fig. 4 that the single-antenna CM detector can still be used, and the two-antenna version still outperforms the mean/max scheme with this GMSK signal. Although not shown for clarity, these ROC curves are almost identical to those obtained with a synthetic, true CM signal.

For comparison, Fig. 4 also shows the ROC curves of both detectors for a white Gaussian signal for $M = 2$ antennas. With this signal, the CM detector can only exploit the spatial independence of noise, and is beaten at this by the mean/max scheme. Also note that the performance of the mean/max detector is almost identical for both types of signals.

6. CONCLUSION

The GLR test for multiantenna detection of Constant Modulus signals in white Gaussian noise of unknown variance has been derived. The test compares favorably with the GLR detector for Gaussian signals, which does not take into account the CM property. Although we have focused on exploiting this CM property together with the spatial independence of the noise, in practice there might be more information available to the spectrum sensor about the primary signal. For example, in the case of the GMSK signal its psd is known (up to a scaling). As a topic for future research, this knowledge should be exploited in order to improve detection power.

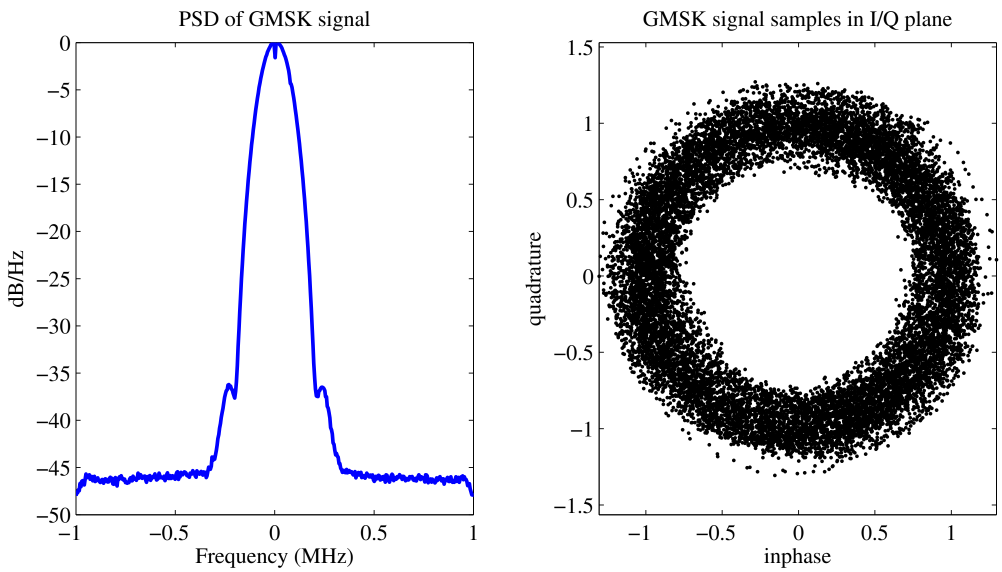

Fig. 3. Power Spectral Density and samples of a GMSK signal.

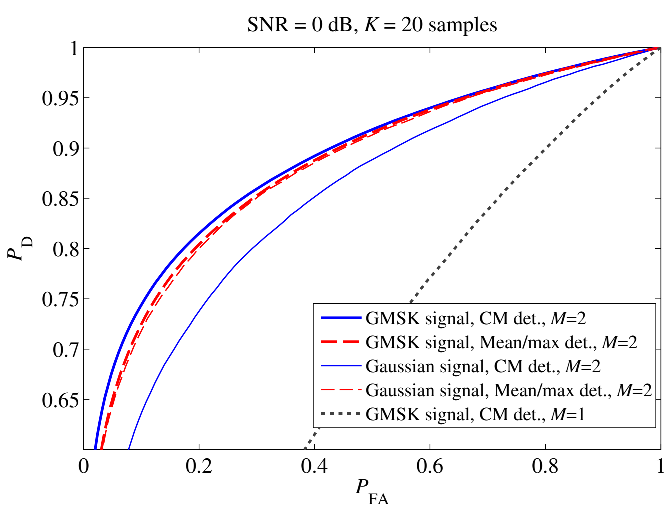

Fig. 4. ROC curves of the CM and mean/max detectors with a GMSK signal and a white complex Gaussian signal.

7. REFERENCES

[1] J. Mitola III, *"Cognitive Radio: an integrated agent architecture for software defined radio,"* Ph.D. Thesis, Royal Institute of Technology, Sweden, May 2000.

[2] D. Čabrić, "Addressing feasibility of cognitive radios," *IEEE Signal Processing Mag.,* vol. 25 no. 6, pp. 85-93, Nov. 2008.

[3] Federal Communications Commission, *"Second report and order for the unlicensed operation in the TV broadcast bands,"* 08-260, Nov. 2008.

[4] J. Treichler and B. Agee, "A new approach to multipath correction of constant modulus signals," *IEEE Trans. Acous. Speech Signal Process.,* vol. 31 no. 2, pp. 459-472, Apr. 1983.

[5] A. Leshem, "Maximum likelihood separation of constant modulus signals," *IEEE Trans. Signal Process.,* vol. 48 no. 10, pp. 2948-2952, Oct. 2000.

[6] M. Derakhtian, A.A. Tadaion, S. Gazor and M.M. Nayebi, " Invariant activity detection of a constant magnitude signal with unknown parameters in white Gaussian noise," *IET Commun.,* vol. 3 no. 8, pp 1420-1431, Aug. 2009.

[7] S. M. Kay, *Fundamentals of statistical signal processing: detection theory*. Englewood Cliffs, NJ: Prentice-Hall, 1993.

[8] R. Tandra, A. Sahai, "SNR walls for signal detection," *IEEE J. Sel. Topics Signal Process.,* vol. 2 no. 1, pp. 4-17, Feb. 2008.

[9] G. Golub, C. van Loan, *Matrix computations, 3rd ed.* London: The Johns Hopkins University Press, 1996.

[10] A. Taherpour, M. Nasiri-Kenari and S. Gazor, "Multiple antenna spectrum sensing in cognitive radios," *IEEE Trans. Wireless Commun.,* vol. 9 no. 2, pp. 814-823, Feb. 2010.

[11] R. López-Valcarce, G. Vazquez-Vilar and J. Sala, "Multiantenna spectrum sensing for cognitive radio: overcoming noise uncertainty," *Proc. 2nd Int. Work. on Cognitive Inform. Process. (CIP)*, June 2010.